OFDM MIMO Space Diversity in Terrestrial Channels

Yuri Labrador, Masoumeh Karimi, Niki Pissinou, and Deng Pan

Florida International University, College of Engineering and Computing

Summary
In this paper, the principles of a MIMO system are analyzed, in addition to how it can be used with OFDM modulation to obtain both frequency and space diversity in a terrestrial multipath Rayleigh channel. Toward this aim, an Alamouti encoder and decoder are employed, in conjunction with QPSK and 16QAM modulation schemes. From the simulation results, it is observed that MIMO, with two transmit and two receive antennas using OFDM and 16QAM, performs well in terms of received BER.

Key words:
MIMO, OFDM, Rayleigh Channel, 16QAM

1. Introduction

One of the most important recent contributions to the study of digital communications has been the adoption of multiple input multiple output (MIMO) techniques. MIMO improves the received signal quality and increases the data communication speed by employing digital signal processing techniques to shape and combine the transmitted signals from multiple wireless paths, created by the use of multiple transmit and receive antennas [1].

In broadband wireless communications, the channel is frequency selective (delay spread), this results in inter-symbol interference (ISI) that can degrade the communication quality. A good technique to mitigate this frequency selective channel is to employ Orthogonal Frequency Division Multiplexing (OFDM). OFDM eliminates the need for high complexity equalization and brings high spectral efficiency. In order to combine the advantages of MIMO and OFDM, space-frequency coded MIMO-OFDM, where two dimensional coding is employed to distribute channel symbols across space (transmitting antennas) and frequency (OFDM carriers) within one OFDM block, can be developed to exploit the available spatial and frequency diversity.

When longer decoding delay and higher decoding complexity are allowable, one may consider coding over several OFDM block periods, resulting in space-time-frequency codes that exploit all of the spatial, temporal and frequency diversity.

Manuscript received October 5, 2009
Manuscript revised October 20, 2009

2. MIMO Systems

Spatial domain diversity can be achieved by using multiple antennas on the transmitter and/or receiver sides. The configuration of multiple antennas can be divided into three categories: (1) MISO (multiple input single output): uses more than one antenna at the transmitter and only one at the receiver; (2) SIMO (single input multiple output): uses one transmitting antenna and more than one receiving antenna; and (3) MIMO: uses more than one antenna at the transmitter and more than one at the receiver.

By using more than one transmit/receive antenna, multiple channels are employed between each pair of transmit and receive antennas (see Figure 1). The transmitted signal will travel through different channels to arrive at the receiver side. If one of the channels is sufficiently strong, the receiver will be able to recover the transmitted signal. If different channels are independent, then the probability of all channels failing is very small.

The greater the number of antennas, the greater the redundancy or diversity of the received signal will be. The low correlation of the different channels can be achieved by separating the antennas at both the transmitter and receiver. The correct antenna separation will depend on the scattering around the neighborhood of the antenna and the channel central frequency. In mobile environments, the separation can range from one-half to one carrier wavelength.

In MIMO systems, both transmit and receive diversities are realized. The overall signal redundancy, or diversity order, is the product of the number of transmit and receive antennas [2]. The MIMO configuration can be realized through design. The designs differ in the antenna configuration at the receiver and transmitter, in addition to the particular form of performance improvement it is designed to obtain. The capacity of a MIMO system increases at least linearly with the minimum number of transmit or receive antennas.

In a MIMO system with M_T transmit antennas and M_R receive antennas, the channel coefficient between transmit antenna i and receive antenna j will be $h_{i,j}$.

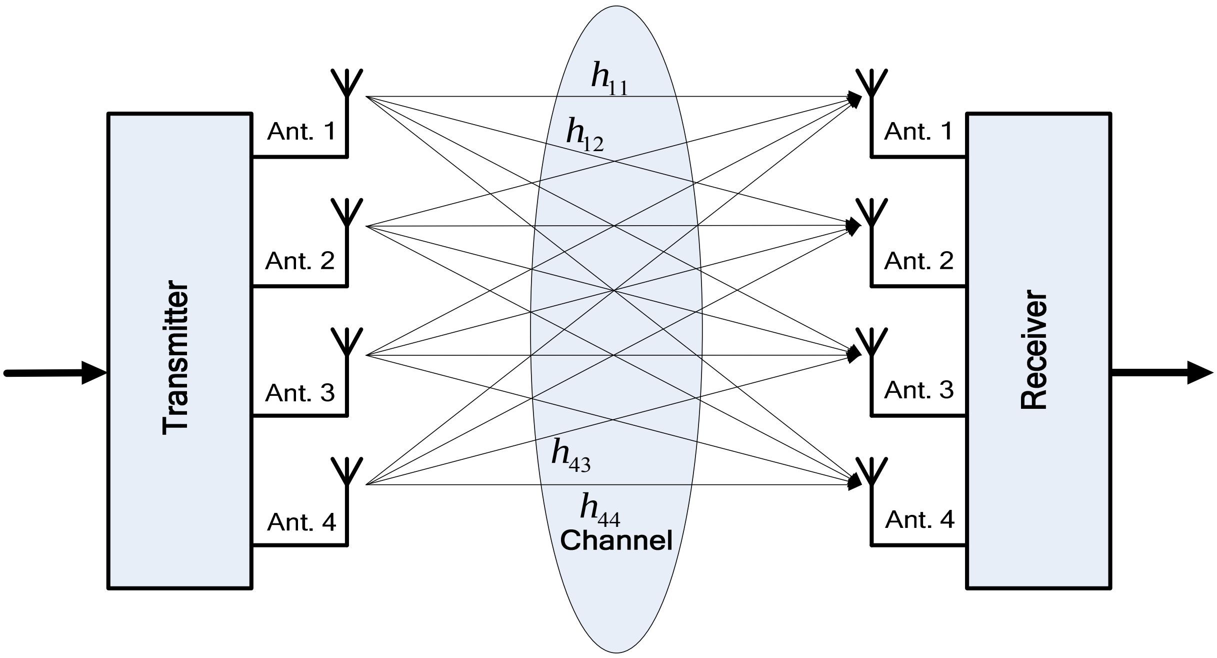

Fig. 1 MIMO Architecture

These h coefficients are modeled as circularly symmetric complex Gaussian random variables, with zero mean and variance equal to one. The MIMO trans-receiver can be modeled by the following equation [1]:

$$Y = \sqrt{\frac{\rho}{M_T}} XH + Z \tag{1}$$

where $X = \lfloor x_1, x_2, ...x_{M_T} \rfloor$ is a signal vector transmitted by the M_T transmit antennas;

$Y = [y_1, y_2, ...y_{M_R}]$ is a signal vector received by the M_R receive antennas; and

$Z = [z_1, z_2, ...z_{M_R}]$ is a noise vector whose elements are modeled as independent circularly symmetric complex Gaussian random variables, with zero mean and variance equal to one.

The channel coefficient matrix $H = \{h_{i,j} : 1 \le i \le M_T, 1 \le j \le M_R\}$ is assumed to be known at the receiver side. The signal vector is assumed to satisfy the energy constraint $E \| X \|_F{}^2 = M_T$, where $\| X \|_F$ is the Frobenius norm of X and defined by:

$$\| X \|_F{}^2 = \sum_{i=1}^{M_T} | x_i |^2 \tag{2}$$

In (1), the factor $\sqrt{\frac{\rho}{M_T}}$ ensures that ρ is the average *SNR* at each receiver antenna, and it is independent of the number of transmitting antennas. If the input signal X is a circularly symmetric complex Gaussian random vector with zero mean and variance $E\{X^H X\}=Q$, then the output signal is also a circularly symmetric complex Gaussian random vector, with zero mean and variance equaling, as follows:

$$E\{Y^H Y\} = \frac{\rho}{M_T} H^H Q \cdot H + I_{M_R} \tag{3}$$

I_{M_T} is an identity matrix of size M_R by M_R. Hence, for any given channel H, the mutual information between the input X and output Y is:

$$I(X;Y \mid H) = \log_2 \det\left(I_{M_T} + \frac{\rho}{M_T} H^H Q \cdot H \right) \tag{4}$$

If the transmitter has no prior knowledge of the channel conditions, each transmitting antenna can be treated equally and allocated the same weight. The variance of the input signal vector over M_T transmit antennas should be an identity matrix. The maximal mutual information will be:

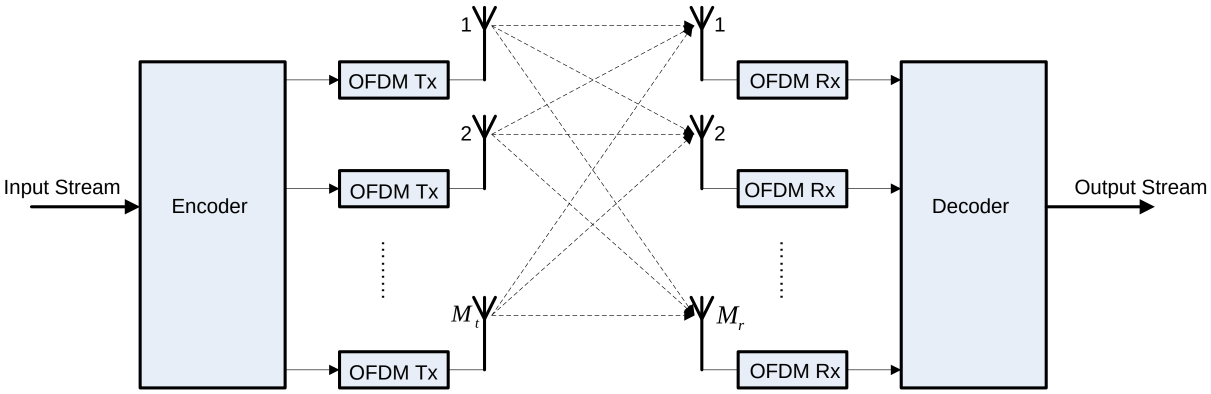

Fig. 2 MIMO-OFDM System

$$\log_2 \det\left(I_{M_R} + \frac{\rho}{M_T} \tilde{H}^H \tilde{H} \right) \qquad (5)$$

If the channel is memory-less, then H changes independently from each use of the channel to another. The average capacity of the MIMO system will be:

$$C = E_H \left\{ \log_2 \det\left(I_{M_R} + \frac{\rho}{M_T} H^H H \right) \right\} \qquad (6)$$

The expectation is taken over the fading channel H. From (5.6), it can be observed that when $M_T = M_R = 1$, the capacity is reduced to a conventional single input single output (SISO) system.

In a MIMO system $M_T = M_R > 1$, for large number of transmitting antennas M_T, the capacity in (5.6) is:

$$C \to \log_2 \det\left(I_{M_R} + \rho \cdot I_{M_R} \right) = M_R \log_2 (1 + \rho) \quad (7)$$

C increases linearly with the number of receiving antennas. The analysis is also true for any systems in which $M_T \geq M_R$. The capacity of a multiple antenna system increases at least linearly with the number of transmit and receive antennas.

3. MIMO-OFDM System

A MIMO-OFDM offers both spatial and frequency diversity in broadband communications. In general, the system is composed of M_T transmitting antennas, M_R receiving antennas, and N OFDM sub-carriers (as indicated in Figure 2). The frequency selective fading channel [3] between each pair of transmit and receive antennas has L independent delay paths and the same power delay profile. The MIMO channel is constant over each OFDM block period [4, 5].

The channel impulse response from transmit antenna i and receive antenna j can be modeled as:

$$h_{i,j} = \sum_{l=0}^{L-1} \alpha_{i,j}(l) \cdot \delta(\tau - \tau_l) \qquad (8)$$

where τ_l is the delay of the lth path, and $\alpha_{i,j}(l)$ is the complex amplitude of the lth path between transmit antenna i and receive antenna j. The time delay τ_l and variance $\delta^2{}_l$ are assumed to be the same for each transmit-receive channel link. The power of the L paths are normalized, such that $\sum_{l=0}^{L-1} \delta^2{}_l = 1$. From (8), the channel frequency response is given by:

$$H_{i,j}(f) = \sum_{l=0}^{L-1} \alpha_{i,j}(l) \cdot e^{-j2\pi \cdot f \cdot \tau_l}, \; j = \sqrt{-1} \qquad (9)$$

The input bit sequence from a channel encoder is divided into b bit long segments, thus forming 2^b source symbols. These symbols are parsed into blocks and mapped onto a space-frequency (SF) code word that is transmitted over the M_T transmit antennas. Each of the SF code words can be defined as a $N \times M_T$ matrix as follows:

$$C = \begin{bmatrix} c_1(0) & c_2(0) & \ldots. & c_{M_T}(0) \\ c_1(1) & c_2(1) & \ldots. & c_{M_T}(1) \\ . & . & . & . \\ . & . & . & . \\ c_1(N-1) & c_2(N-1) & \ldots. & c_{M_T}(N-1) \end{bmatrix} \qquad (10)$$

$c_i(n)$ denotes the channel symbol transmitted over the nth sub-carrier by antenna i, and N is the number of sub-carriers in the OFDM scheme. The OFDM transmitter applies an N point IFFT to each column of the matrix C. After adding a cyclic prefix, the OFDM symbol corresponding to the ith $(i = 1,2,.....M_T)$ column of C is transmitted by transmit antenna i. All of the M_T OFDM symbols are transmitted at the same time from different transmit antennas.

At the receiver, after filtering, removing the cyclic prefix, and applying FFT, the received signal at the nth sub-carrier at receive antenna j is:

$$y_j(n) = \sqrt{\frac{\rho}{M_T}} \sum_{i=1}^{M_T} c_i(n) \cdot H_{i,j}(n) + z_j(n) \qquad (11)$$

where $$H_{i,j}(n) = \sum_{l=0}^{L-1} \alpha_{i,j}(l) \cdot e^{-j2\pi \cdot n\Delta f \cdot \tau_l} \qquad (12)$$

is the channel frequency response at the nth sub-carrier between transmit antenna i and receive antenna j, $\Delta f = \frac{1}{T}$ is the sub-carrier separation in frequency domain, and T is the OFDM symbol period. The channel state information $H_{i,j}(n)$ is known at the receiver, but not at the transmitter. The term $z_j(n)$ in (11) denotes the additive complex Gaussian noise with zero mean and variance of one at the nth sub-carrier at receive antenna j. The noise samples $z_j(n)$ are uncorrelated for different values of *j* and *n*.

The factor $\sqrt{\frac{\rho}{M_T}}$ guarantees that ρ is the average SNR at each receive antenna, independent of the number of transmit antennas [6].

4. Terrestrial Channel Model

In the terrestrial channel, the signal also travels many paths. The signal reaching the mobile user is formed by the sum of these different paths. The terrestrial channel is formed in this analysis by the relay node and the mobile user, which will be explained in further detail in Chapter 6. This section instead focuses on the terrestrial channel model. As mentioned above, the signal reaching the receiver is the sum of many constructive and destructive paths. The receiver perceives this as a variation of the amplitude, phase and angle of the arrival signal. The received signal will be a set of attenuated, time-delayed, phase-shifted replicas of the transmitted signal. Fading is divided in two groups: (1) large-scale fading, which means variations over large distances, and (2) small-scale fading, including the effects of small changes in the separation between the transmitter and receiver.

These variations can be caused by the mobility of the transmitter, the receiver or the intermediate objects in the path of the signal [7]. A non-deterministic model for the phenomenon exists and is thus characterized statistically. If there is no direct LOS between the transmitter and receiver, the Rayleigh distribution approximates the channel envelope, and the fading is known as Rayleigh fading. Figure 3 shows a model representation with a transmitter antenna and a mobile user.

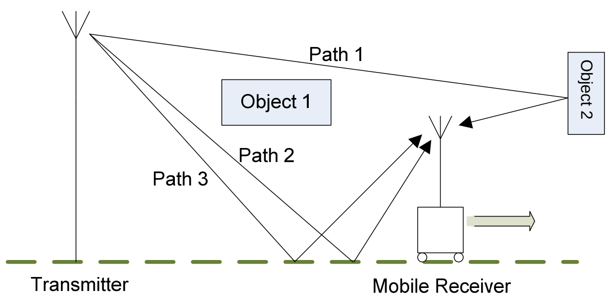

Fig. 3 Terrestrial Rayleigh Model

Small-scale fading can be separated into two types – frequency selective fading and frequency non-selective fading. Frequency non-selective fading is also known as flat fading because all frequency components of the transmitted signal are affected by the channel response. In flat fading, the effect of the channel over the transmitted signal can be represented through a low pass equivalent of the channel response [8].

$$h(t) = h_{phase}(t) + jh_{quadrature}(t) \qquad (13)$$

The phase and quadrature components are independent of each other and Gaussian-distributed. The envelope of the fading channel is Rayleigh-distributed, expressed as:

$$r(t) = \sqrt{h^2{}_{phase} + h^2{}_{quadrature}} \qquad (14)$$

The instantaneous SNR at the receiver, $SNR(t)$, is used as an indicator of the channel state at a given time. When the channel is poor, the signal will be severely degraded over the channel and the SNR will be low. Conversely,

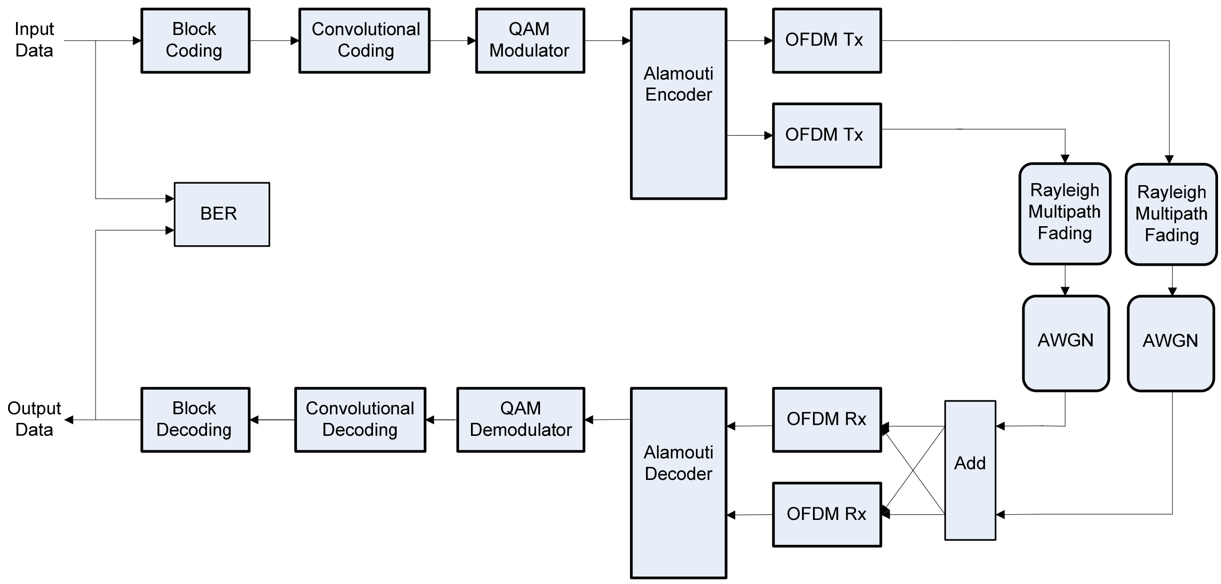

Fig. 4 MIMO OFDM Simulation Block Diagram

when the channel is strong, the signal can be detected easily at the receiver; thus, its SNR will be high. The instantaneous SNR is related to the channel response as follows:

$$SNR(t) = |h(t)|^2 \frac{E_S}{N_O} \tag{15}$$

where E_S is the average energy per symbol, and N_O is the noise power spectral density. If the noise is Additive White Gaussian Noise (AWGN), then $SNR(t)$ is exponentially distributed for Rayleigh channels.

The coherence time of the channel is the time over which the channel response can be considered invariant, given by the following equation:

$$T_C = \frac{1}{f_D} \tag{16}$$

where f_D is the Doppler frequency, the maximum frequency shift due to the relative movement of the transmitter and receiver. The autocorrelation function represents the variability of the channel over time. It depends on the propagation geometry, the velocity of the mobile and the antenna characteristics. The isotopic scattering is commonly assumed, meaning that the channel consists of many scatterers that are densely packed with respect to the angle. This is usually referred to as the "classical model." The channel impulse response is a wide-sense stationary (WSS), and the continuous time autocorrelation function (ACF) of the phase and quadrature components does not depend on time, but on the time difference, τ .

$$R_{h_{phase}}(\tau) = R_{h_{quadrature}}(\tau) = b_0 \cdot J_0(2\pi \cdot f_D \cdot \tau) \tag{17}$$

J_0 is the zeroth order Bessel function of the first kind, and f_D is the maximum Doppler frequency.

In the discrete time domain, it is better to express the Doppler frequency normalized by the sampling rate, multiplied by the symbol period $T_S (f_D \cdot T_S)$. Low values of $(f_D \cdot T_S)$ indicate high correlation in the signal, and conversely, high values of the product $(f_D \cdot T_S)$ mean low correlation in the signal. In the limit $(f_D \cdot T_S) \rightarrow \infty$, there is no correlation, and the samples are independent of one another. If the envelope is a Rayleigh, the expression of the ACF can be defined as:

$$R_r(\tau) = \frac{\pi \cdot b_0}{2} F_1\left(-\frac{1}{2}, -\frac{1}{2}; \left(J_0\left(2\pi \cdot f_D \tau\right)\right)^2\right) \tag{18}$$

5. Simulation Results

Figure 4 shows the simulation block diagram in MatLab used to model the terrestrial channel MIMO OFDM link. The input random bits are fed into a block coding block,

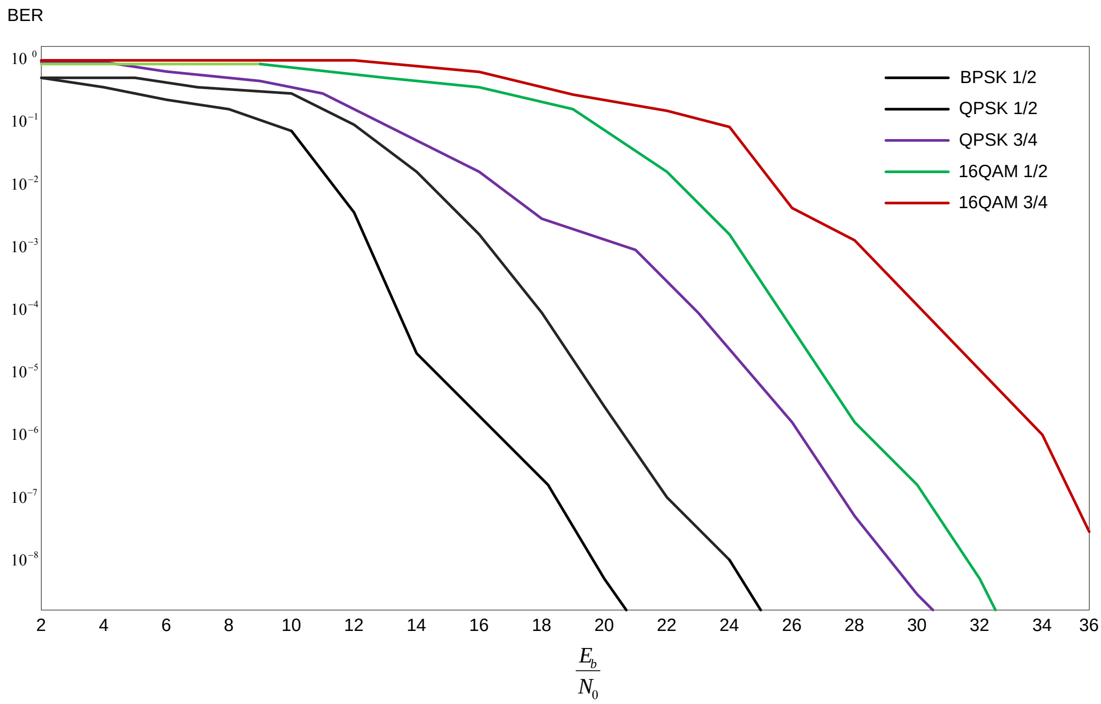

Fig. 5 $\frac{E_b}{N_0}$ versus BER Results for BPSK, QPSK and 16QAM

which adds redundant bits in order to perform channel block coding. This block converts the input bits into blocks of fixed length and adds redundant bits to each block, so its output block will be longer than the input block.
The output of the block coding is fed into a convolutional coding block that performs another type of channel coding, known as the Trellis algorithm. This type is different from block coding, in that the input bits are not divided into blocks of fixed length; instead, the input bits are encoded continuously. The combination of block codes and convolutional codes allows a robust combination when detecting and correcting errors at the receiver, which uses a Viterbi decoder to decode the Trellis algorithm and a block decoding to decode the block codes. This process is known as concatenated coding.

The output of concatenated coding is modulated using a QAM modulator, and then fed into an Alamouti encoder to perform the MIMO technique, in this case, a 2x2 system. The 2x2 system uses two transmit and two receive antennas that perform the space diversity. The Alamouti encoder outputs are modulated using two OFDM transmitters and two antennas, which transmit the OFDM signal through a Rayleigh multipath channel.

The simulation parameters are the following:

Bandwidth: 5 MHz
Central frequency: 1.5 GHz
OFDM sub-carrier spacing: Δf = 15 KHz
OFDM IFFT size: 2048 for 16QAM
OFDM IFFT size: 1024 for QPSK
Number of OFDM symbols: 12
Cyclic prefix duration: 16.67 μs
Maximum Doppler shift: 15 Hz
Error correction rates:
- BPSK: ½
- QPSK: ½, ¾
-16QAM: ½, ¾
- 64QAM: 2/3
Number of transmit antennas: 2
Number of receive antennas: 2
Channel type: Multipath Rayleigh Fading
Block coding: 188/204

Above, Figure 5 shows the functions of $\frac{E_b}{N_0}$ versus BER for different modulations and error correction codes. BPSK ½ shows the best performance, compared to the others modulation schemes, but it lacks the capacity to transmit high data rates. QPSK ½ and QPSK ¾ can accommodate larger data rates, and their BER performances are good in Rayleigh fading channels with OFDM transmissions.

16QAM ½ can perform with acceptable BER values over Rayleigh channels, and it is capable of carrying high data rates, depending on the error correction code that is selected. The figure shows that BER is better with 16QAM ½, compared to 16QAM ¾. This is because with ½, the number of redundant bits is considerably higher than in the 16QAM ¾ case. However, even with the high amount of redundant bits, 16QAM ½ is capable of accommodating high data rates needed in 4G systems.

The following tables show the results for all the cases presented in Figure 5.

Table 1 BER BPSK ½ *BW= 5 MHz*

$\frac{E_b}{N_0}[dB]$	**Bit Error Rate BER**
4	.465
6	.402
8	.209
10	.0182
12	.00039
14	$2.14\,e^{-5}$
16	$3.25\,e^{-6}$
18	$4.37\,e^{-7}$
20	$1.75\,e^{-8}$

Table 2 BER QPSK ½ *BW= 5 MHz*

$\frac{E_b}{N_0}[dB]$	**Bit Error Rate BER**
8	.458
10	.445
12	.295
14	.064
16	.0025
18	$1.74\,e^{-5}$
20	$1.23\,e^{-6}$
22	$3.49\,e^{-7}$
24	$5.26\,e^{-8}$

Table 3 BER QPSK ¾ *BW= 5 MHz*

$\frac{E_b}{N_0}[dB]$	**Bit Error Rate BER**
6	.486
8	.484
10	.476
12	.462
14	.443
16	.354
18	.165
20	.0242
22	.0009
24	$7.48\,e^{-5}$
26	$5.95\,e^{-6}$
28	$6.83\,e^{-7}$
30	$3.48\,e^{-8}$

Table 4 BER 16QAM ½ *BW= 5 MHz*

$\frac{E_b}{N_0}[dB]$	**Bit Error Rate BER**
6	.495
8	.483
10	.482
12	.481
14	.476
16	.457
18	.325
20	.127
22	.01243
24	.00035
26	$4.92\,e^{-5}$
28	$3.94\,e^{-6}$
30	$4.36\,e^{-7}$
32	$5.64\,e^{-8}$

Table 5 BER 16QAM ¾ *BW= 5 MHz*

$\frac{E_b}{N_0}[dB]$	**Bit Error Rate BER**
6	.492
8	.495
10	.491
12	.482
14	.481
16	.480
18	.475
20	.444
22	.394
24	.337
26	.0095
28	.0047

30	.00031
32	$4.83\,e^{-5}$
34	$2.32\,e^{-6}$
36	$8.78\,e^{-7}$
38	$5.44\,e^{-8}$

The signal spectrum for the OFDM 16QAM transmitted by Antennas 1 and 2 are shown in Figure 6. The received spectrum is shown in Figure 7; note the signal attenuation due to the Rayleigh channel.

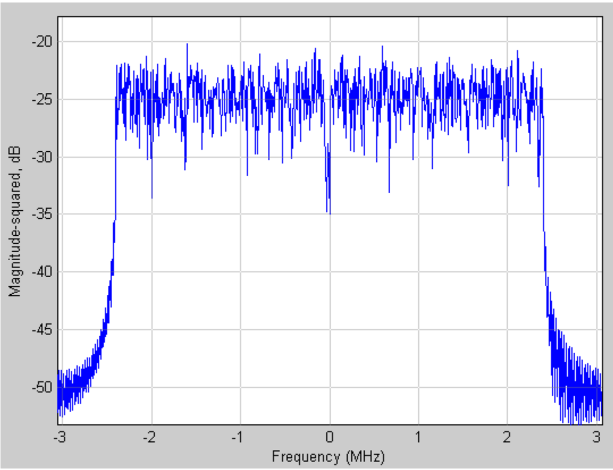

Fig. 6 OFDM 16QAM ¾ Transmitted Spectrum Antenna 1

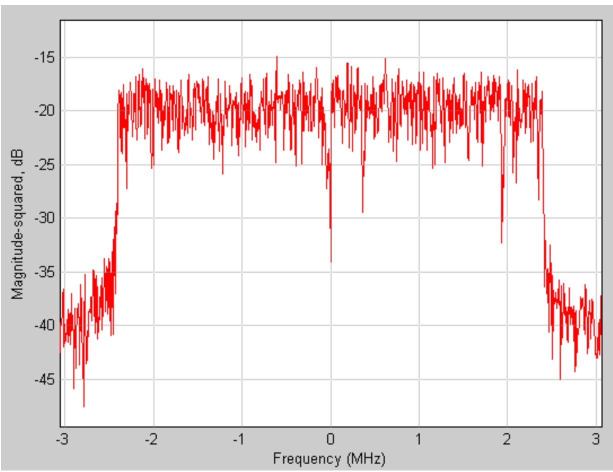

Fig. 7 OFDM 16QAM ¾ Received Spectrum BER = 4.83 e^{-5}

The 16QAM and QPSK transmitted and received constellations are shown in Figures 8 and 9, respectively.

Note that the noise affects the phases more prominently in 16QAM due to the phase's proximity.

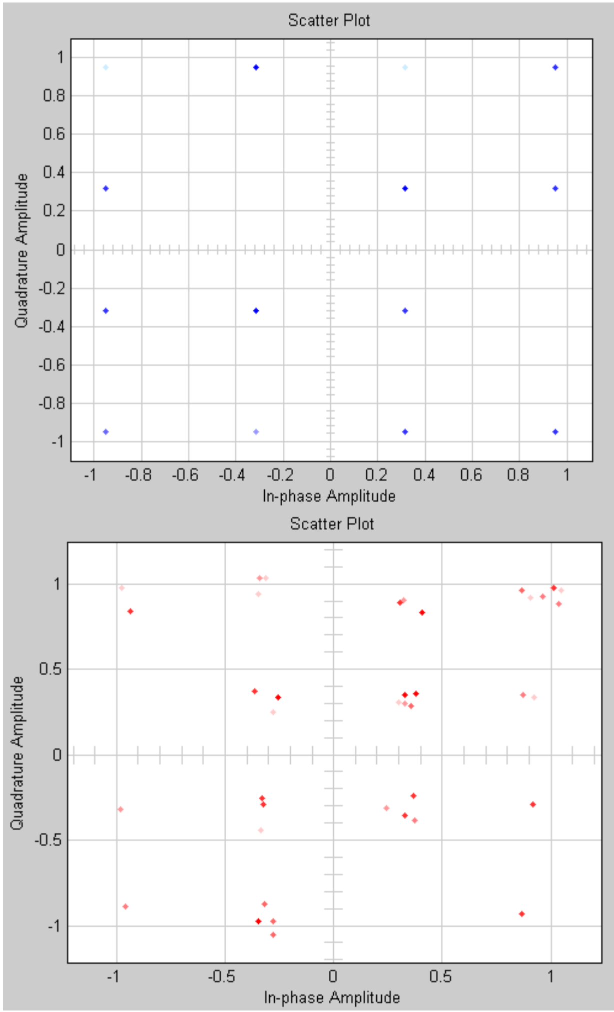

Fig. 8 16QAM ¾ Transmitted (Blue) and Received (Red) Constellations BER = 4.83 e^{-5}

In addition, the signal eye diagram for QPSK and 16QAM modulations can be found in Figures 10 and 11.

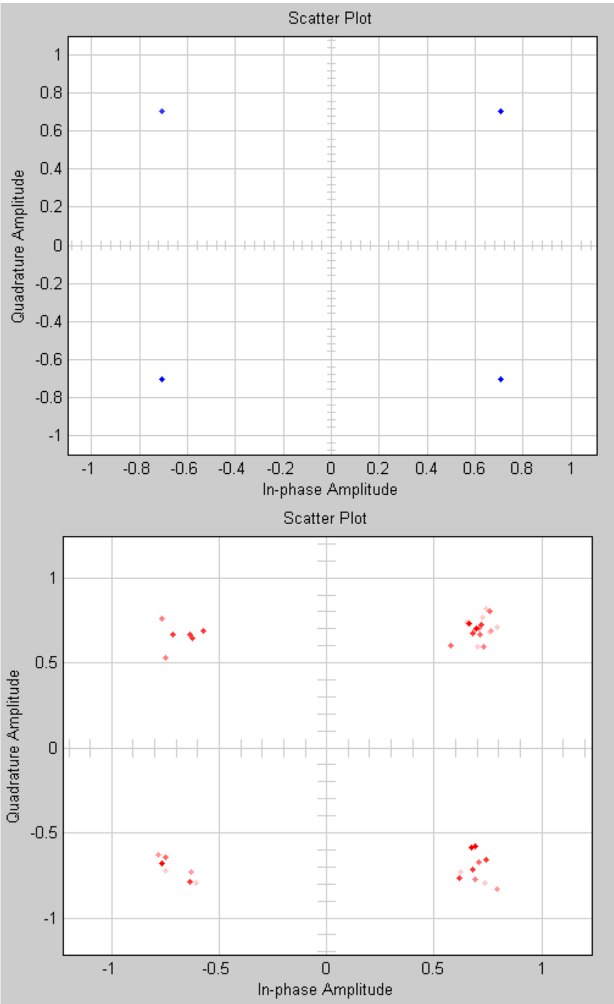

Fig. 9 QPSK ¾ Transmitted and Received Constellations BER = $7.48\, e^{-5}$

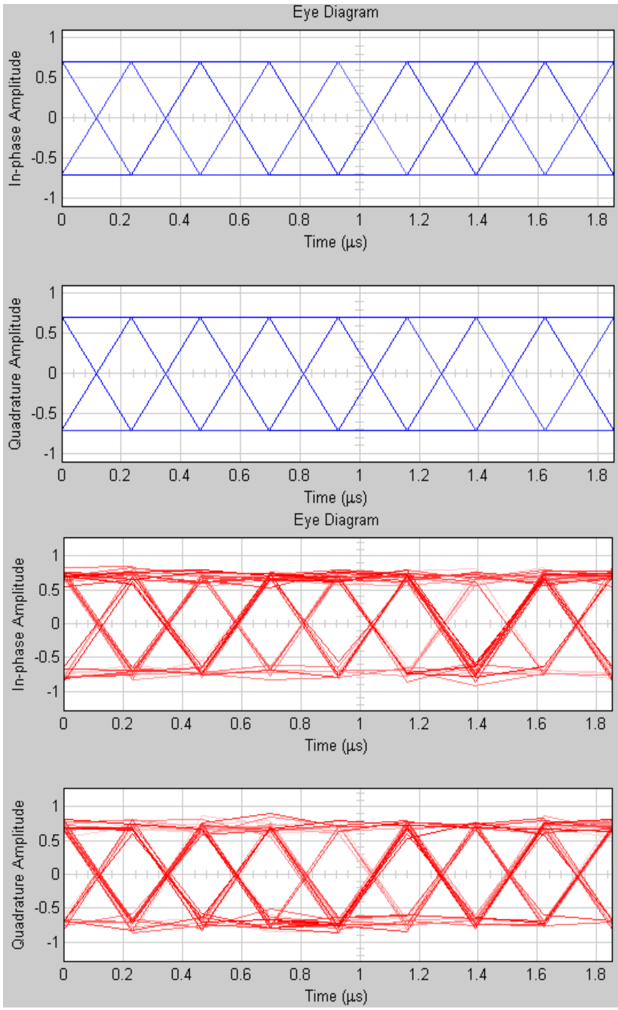

Fig. 10 QPSK ¾ Transmitted (Blue) and Received (Red) Eye Diagrams BER = $7.48\, e^{-5}$

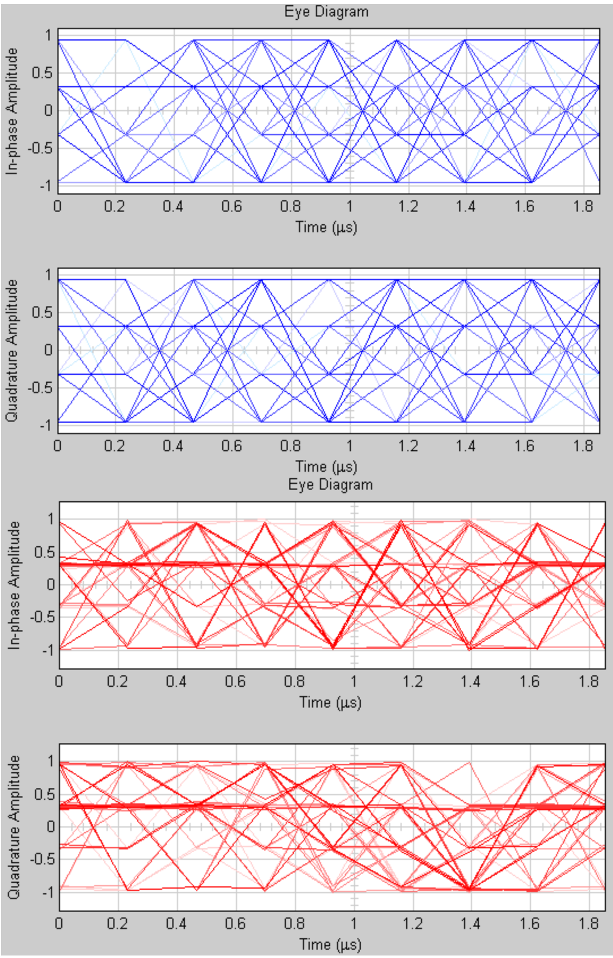

Fig. 11 16QAM ½ Transmitted and Received Eye Diagrams BER = $3.94\,e^{-6}$

6. Conclusions

In this work, the principles of a MIMO system were analyzed, in addition to how it can be used with OFDM modulation to obtain both frequency and space diversity in a terrestrial multipath Rayleigh channel. Toward this aim, an Alamouti encoder and decoder were employed, in conjunction with QPSK and 16QAM modulation schemes. From the simulation results, it is observed that MIMO, with two transmit and two receive antennas using OFDM and 16QAM, performs well in terms of received BER. The values shown in Tables 4 and 5 were obtained using MatLab version 7.6.0.324.

References

[1] K. J. Ray Liu, Ahmed K. Sadek, Weifeng Su, and Andres Kwasinski. "Cooperative Communications and Networks," Cambridge, ISBN 978-0-521-89513-2, January 2009.

[2] J. C. Guey, M. P. Fitz, M. R. Bell, and W. Y. Kuo. "Signal design for transmitter diversity wireless communications systems over Rayleigh fading channels," IEEE Transactions on Communications, 47: pp. 527-537, April 1999.

[3] Z. Liu, Y. Xin and G. Giannakis. "Space time frequency coded OFDM over frequency selective fading channels," IEEE transaction on Signal Processing, 50: pp. 2465-2476, October 2002.

[4] B. Lu and X. Wang. "Space time code design in OFDM systems," In Proceedings of the IEEE Global Telecommunications Conference, GLOBECOM'00, pp. 1000-1004, 2000.

[5] B. Lu, Wang and K. R. Narayanan. "LDPC based space time coded OFDM systems over correlated fading channels: performance analysis and receiver design," IEEE Transaction on Communications, 50(1): pp. 74-88, January 2002.

[6] A. Shokrollahi, B. Hassibi, B. M. Hochwall, and W. Sweldens. "Representation theory for high rate multiple antenna code design," IEEE Transactions on Information Theory, 47: pp. 2335-2367, September, 2001.

[7] T. S. Rappaport, "Wireless Communications: Principles and Practice," Prentice Hall, Inc. Upper Saddle River, New Jersey, 1996.

[8] J. G. Ruiz, B. Soret, Aguayo-Torres, M. Carmen, J. T. Entrambasaguas, "On finite state Markov chains for Rayleigh channel modeling," 1st International Conference on Wireless Communication, Vehicular Technology, Information Theory and Aerospace & Electronic Systems Technology (WIRELESSVITAE), pp. 191-195, 2009.